

^8Be Nuclear Data Evaluation

Philip R. Page and Gerald M. Hale¹

Theoretical Division, MS B283, Los Alamos National Laboratory, Los Alamos, NM 87545, USA

Abstract.

An R-matrix analysis of experimental nuclear data on the reactions $^4\text{He}(\alpha, \alpha)$, $^4\text{He}(\alpha, p)$, $^4\text{He}(\alpha, d)$, $^7\text{Li}(p, \alpha)$, $^7\text{Li}(p, p)$, $^7\text{Li}(p, n)$, $^7\text{Be}(n, p)$, $^6\text{Li}(d, \alpha)$, $^6\text{Li}(d, p)$, $^6\text{Li}(d, n)$ and $^6\text{Li}(d, d)$, leading to the ^8Be intermediate state, has been completed in the last two years. About 4700 data points from 69 experimental references are included. The excitation energy above the ^8Be ground state is 25 – 26 MeV for all reactions except $^4\text{He}(\alpha, \alpha)$ and $^7\text{Be}(n, p)$. The data for the reactions $^4\text{He}(\alpha, \alpha)$ and $^6\text{Li}(d, d)$ do not fit well, but the other reactions fit with a $\chi^2/(\text{point})$ of less than the overall value of 7.9. Most of the 19 resonances found in the R-matrix analysis correspond to resonances formerly known from experiment. Evaluated integrated $^4\text{He}(\alpha, p)$, $^4\text{He}(\alpha, d)$, $^7\text{Li}(p, \alpha)$, $^7\text{Li}(p, n)$, $^7\text{Be}(n, p)$, $^6\text{Li}(d, \alpha)$, $^6\text{Li}(d, p)$ and $^6\text{Li}(d, n)$ reaction cross-sections are presented. Evaluated cross-section and angular dependence files in ENDF format were prepared for the twelve reactions $p^7\text{Li}$, $n^7\text{Be}$, $d^6\text{Li} \rightarrow \alpha^4\text{He}$, $p^7\text{Li}$, $n^7\text{Be}$, $d^6\text{Li}$. Maxwellian averaged temperature-dependent cross-sections in NDI format were prepared for the six reactions $^7\text{Li}(p, \alpha)$, $^7\text{Li}(p, n)$, $^7\text{Be}(n, p)$, $^6\text{Li}(d, \alpha)$, $^6\text{Li}(d, p)$ and $^6\text{Li}(d, n)$.

This analysis of two-body strong reactions leading to the ^8Be intermediate state was motivated by large discrepancies between various evaluations.

There are 16 different reactions for which cross-sections have been obtained via this analysis. These are $\alpha^4\text{He}$, $p^7\text{Li}$, $n^7\text{Be}$, $d^6\text{Li} \rightarrow \alpha^4\text{He}$, $p^7\text{Li}$, $n^7\text{Be}$, $d^6\text{Li}$. In addition to unitarity, constraints between reactions are also provided by time-reversal symmetry (i.e. when the initial and final particles are interchanged), and isospin symmetry. For example, no data were entered for $^4\text{He}(\alpha, n)$, $^7\text{Li}(p, d)$, $^7\text{Be}(n, \alpha)$, $^7\text{Be}(n, n)$ and $^7\text{Be}(n, d)$; and only very low energy data for $^7\text{Be}(n, p)$. However, three of these reactions are strongly constrained via their time-reverse reactions [$^7\text{Li}(p, d)$, $^7\text{Be}(n, d)$ and $^7\text{Be}(n, p)$]. Moreover, the other three reactions are constrained by isospin symmetry [$^4\text{He}(\alpha, n)$ is constrained by $^4\text{He}(\alpha, p)$, $^7\text{Be}(n, \alpha)$ by $^7\text{Li}(p, \alpha)$, and $^7\text{Be}(n, n)$ by $^7\text{Li}(p, n)$].

Integrated, differential and polarization cross-section data were entered for the eleven reactions listed in the abstract. Substantial data were entered for the $^4\text{He}(\alpha, \alpha)$ and $^7\text{Li}(p, p)$ reactions, and the least data were entered for the $^4\text{He}(\alpha, p)$, $^4\text{He}(\alpha, d)$ and $^6\text{Li}(d, d)$ reactions. All reactions where data were entered, except $^4\text{He}(\alpha, \alpha)$ and $^7\text{Be}(n, p)$, include data up to an excitation energy of 25 – 26 MeV. In the $^4\text{He}(\alpha, \alpha)$ reaction, data above the maximum α laboratory energy for which data were entered (38.4 MeV) and below the limit of this analy-

sis (52 MeV laboratory energy), are only available as phase shifts [2], and have not been incorporated. For the $^7\text{Be}(n, p)$ reaction no data above the near-threshold data entered were found below the maximum excitation energy of this analysis (26 MeV).

Cross-sections for the seven reactions mentioned in the abstract in the energy range corresponding to the excitation energy of this analysis are shown in Figs. 1-3. The cross-sections are in barns or millibarns, as indicated; the energies are the laboratory energies of the projectile. Only the integrated cross-section data that were entered are indicated. The cross-sections for $^7\text{Li}(p, \alpha)$ and $^6\text{Li}(d, \alpha)$ in the Figs. 2-3 should be divided by 2 to obtain reaction cross-sections, since there are identical final particles. The shape of the $^4\text{He}(\alpha, p)$ (Fig. 1) reaction is driven by the time-inverse $^7\text{Li}(p, \alpha)$ (Fig. 2) reaction, which has much more data. Similarly, the shape of the $^4\text{He}(\alpha, d)$ (Fig. 1) reaction is driven by the time-inverse $^6\text{Li}(d, \alpha)$ (Fig. 3) reaction. Also, the shape of the $^6\text{Li}(d, n)$ (Fig. 3) reaction is driven by the $^6\text{Li}(d, p)$ (Fig. 3) reaction: the isospin 0 components of these reactions are related by isospin symmetry. The magnitude and shape of the $^7\text{Li}(p, n)$ cross-section from 3 – 7 MeV have changed considerably at various stages of the analysis, so that further investigation of this reaction is needed.

REFERENCES

1. P.R. Page, " ^8Be Nuclear Data Evaluation", LA-UR-04-7172, pp. 1-35.
2. A.D. Bacher *et al.*, *Phys. Rev. Lett.* **29**, 1331 (1972).

¹ E-mail: prp@lanl.gov, ghale@lanl.gov

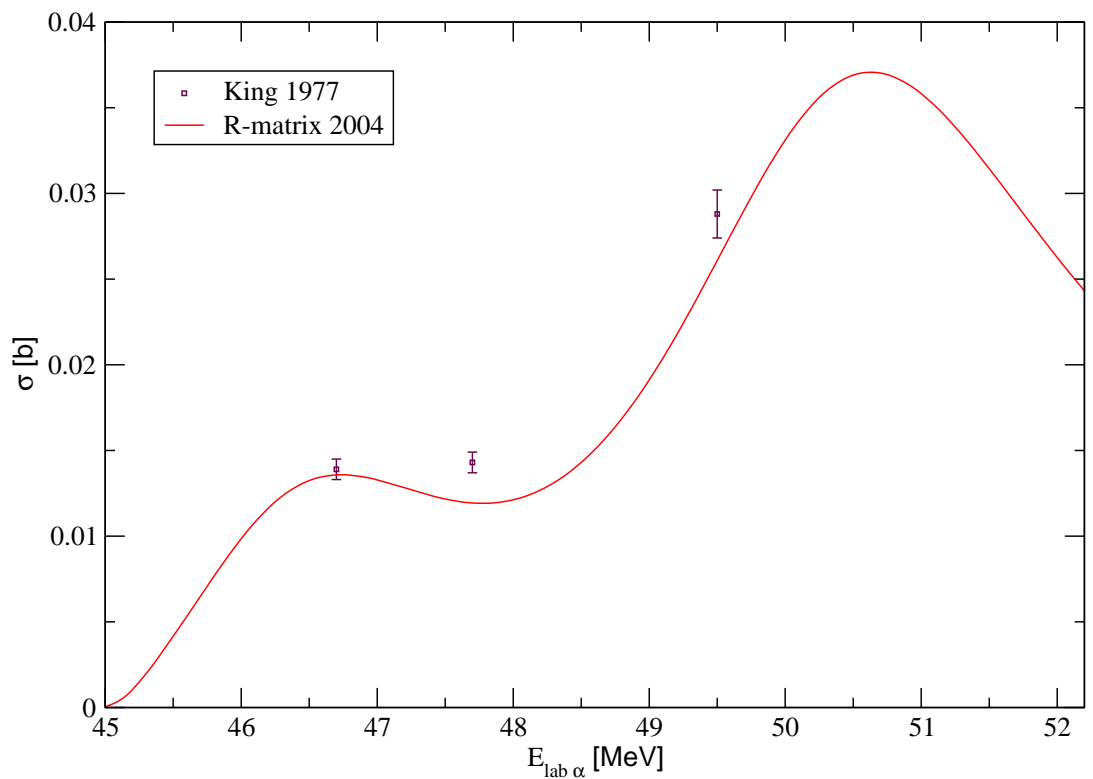
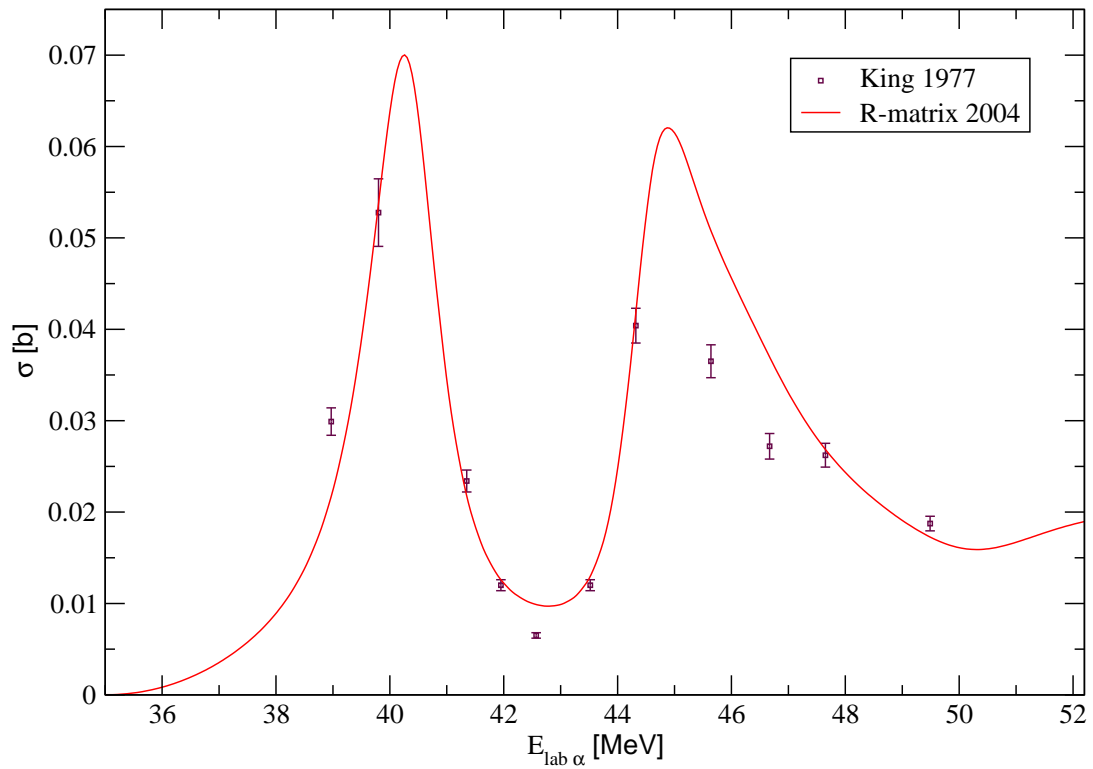


FIGURE 1. From top to bottom: Evaluated 2004 R-matrix cross-sections and experimental data for (a) ${}^4\text{He}(\alpha,p)$ and (b) ${}^4\text{He}(\alpha,d)$.

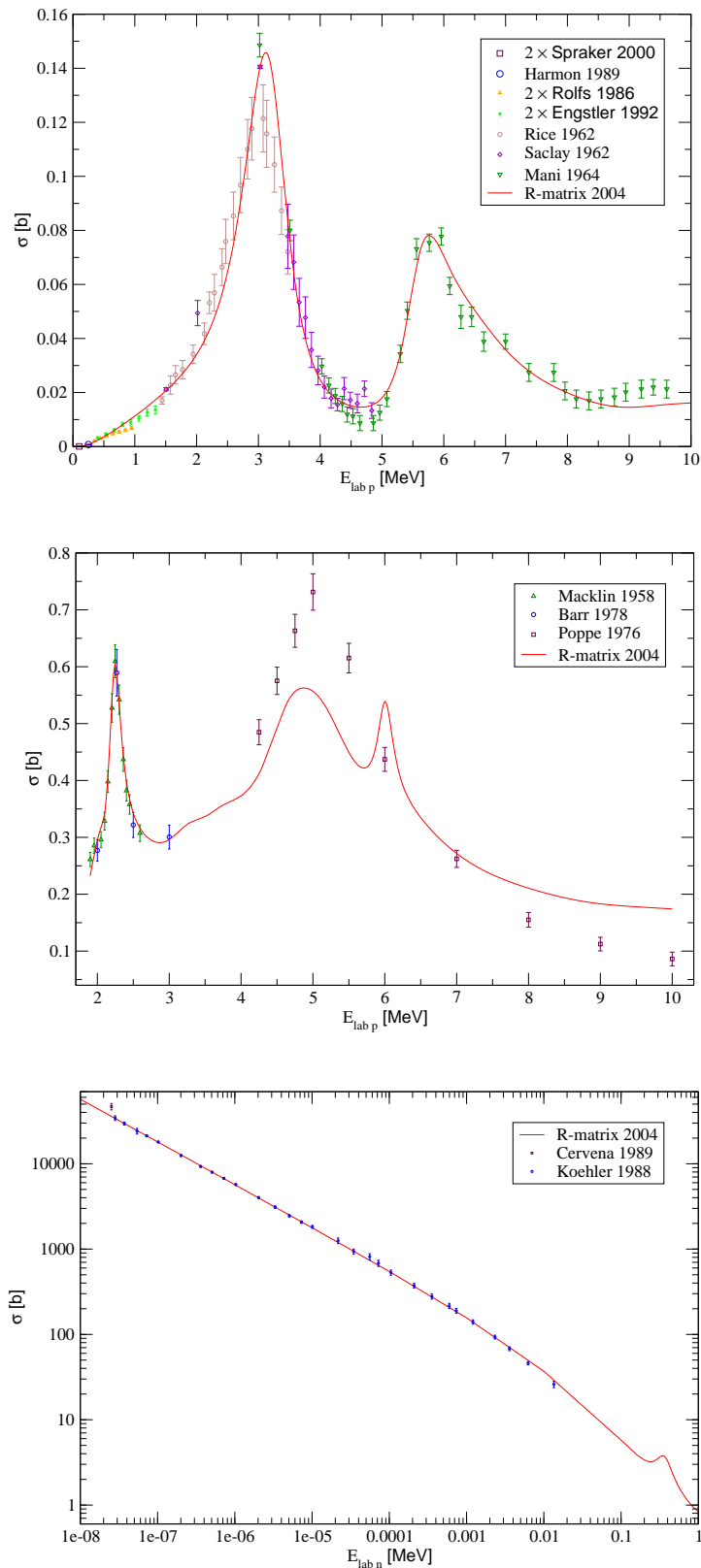


FIGURE 2. From top to bottom: Evaluated cross-sections for (a) ${}^7\text{Li}(p, \alpha)$, (b) ${}^7\text{Li}(p, n)$ and (c) ${}^7\text{Be}(n, p)$.

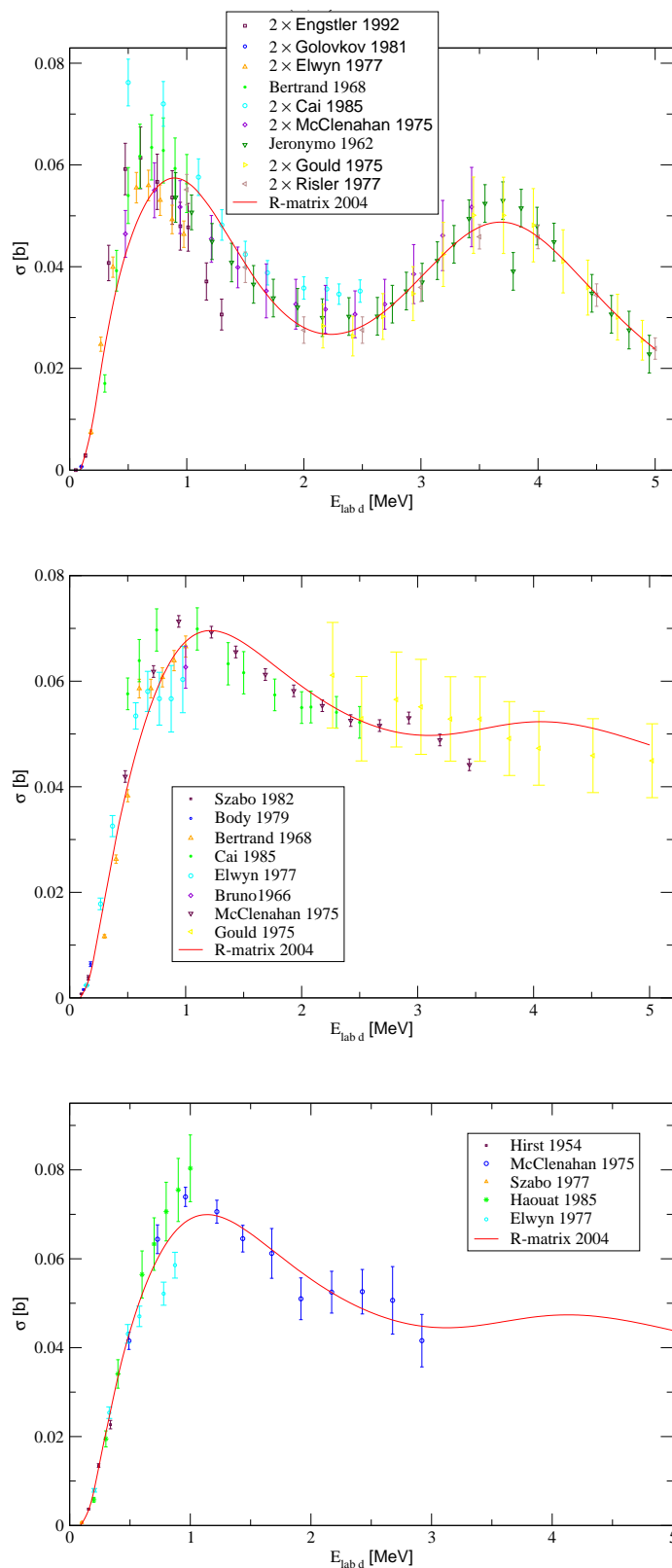


FIGURE 3. From top to bottom: Evaluated cross-sections for (a) ${}^6\text{Li}(d, \alpha)$, (b) ${}^6\text{Li}(d, p)$ and (c) ${}^6\text{Li}(d, n)$.